Nonconvex interactions: A mechanism for the occurrence of modulated order in condensed matter

Mario Marchand,* Kevin Hood, and Alain Caillé

Département de Physique et Centre de Recherche en Physique du Solide, Université de Sherbrooke, Sherbrooke, Québec, Canada J1K 2R1

(Received 14 August 1987)

We present a detailed analysis of one-dimensional models where frustration results from the presence of nonconvex interparticle interactions. The phase diagrams, obtained numerically, are qualitatively different depending on whether or not the particles, in the ground state, experience the nonconvex part of the interaction potential. When the particles experience only the convex part of the interaction potential, only phases where the *winding number* is uniquely defined are found and the transitions among these phases are suggestive of a complete devil's-staircase behavior. When some of the particles, in the ground state, experience the nonconvex part of the interaction potential, phases where the winding number is not uniquely defined are found. In this case, both first- and second-order phase transitions and possibly quasicontinuous transitions are found. Also of interest is the existence of sequences of superdegenerate points where the system has residual entropy and violates the third law of thermodynamics. At these points, we show that the ground state consists of noninteracting solitons of zero energy.

I. INTRODUCTION

Today, many materials are known to exhibit phases which are characterized by a commensurate or incommensurate spatial modulation of a local property such as magnetization, electric polarization, charge and mass density, or chemical composition.[1] Usually, the occurrence of these phases is looked for in the ground state of a given Hamiltonian or mean-field free energy. In that respect, the two most popular theoretical models have certainly been the Frenkel-Kontorova[2] model and the axial next-nearest-neighbor (ANNNI) model.[3-6]

In the Frenkel-Kontorova model, frustration results from the competition between two periodicities: the equilibrium length of the first-neighbor harmonic interaction, and the period of the sinusoidal substrate potential. On the other hand, in the ANNNI model (within mean-field theory), frustration occurs when the following ingredients are present simultaneously: competing first- and second-neighbor harmonic interactions and a temperature-dependent double-well potential to which the continuous variables (representing the average magnetization of a plane) are submitted. In that respect, the models of Axel and Aubry[7] and Janssen and Tjon[8] are quite similar to the ANNNI model, since they both contain all of these ingredients. The only differences concern the mathematical form of the double-well potential and the "physical" significance of the continuous degrees of freedom (namely, they represent displacements of atoms in the case of Axel and Aubry but they are bond variables in the model of Janssen and Tjon).

Recently, in a short paper,[9] we proposed a different mechanism for the occurrence of modulated order in condensed matter. The model consists of particles submitted to a convex (i.e., with monotonously increasing

first derivative) substrate potential and interacting with their first neighbors through a *nonconvex* interaction potential. It is easy to show that frustration leading to periodically modulated ground states can only occur in this model when the interparticle interaction potential is nonconvex. Similar to the ANNNI model (and related models) but contrary to the Frenkel-Kontorova model, the ground state can only occur in the thermodynamic limit with zero average lattice distortion. On the other hand, as in the Frenkel-Kontorova model but contrary to the ANNNI model, only first-neighbor interactions are present and are needed to obtain modulated ground states. In this paper we investigate the complicated structure of the phase diagram for such a model.

The motivation for this kind of study is twofold. Firstly, nonconvex interactions are common in solid state physics. The oscillating (Ruderman-Kittel-Kasuya-Yoshida) exchange interaction between localized spins in a metal is perhaps the most famous example. Also, it has been shown[10] recently that magnetoelastic coupling leads to an effective double-well interparticle interaction. More generally, and relevant to ferroelectricity, Villain and Gordon[11] have shown that oscillating (and hence nonconvex) interactions can be mediated through elastic strains and other harmonic fields. The second reason that motivates this study is that nonconvex effects are presently far from well understood. This is not surprising, since theoretical approaches to problems involving nonconvex interparticle interactions have so far been limited to models where frustration (leading to modulated ground states) is present, even when the interparticle interactions are convex. For example, if we replace the interaction terms of the models studied by Aubry, Fesser, and Bishop,[12] Banerjea and Taylor,[13] and Yokoi, Tang, and Chou[14] by convex harmonic interactions, we recover the Frenkel-Kontorova model. Hence,

in order to focus only on nonconvex effects, we have decided to study microscopic models having nonconvex interactions and for which the ground state is always uniform (unmodulated) when these interactions are convex. Furthermore, these chosen models are representative of certain kinds of interactions that can occur in real solids. In fact, they are related to certain magnetoelastic problems[10] (more details will be given in a later publication) and, as shown by Kholopov,[15] may be suited to describe phase transitions in ferroelectrics such as $TlHF_2$.

In our opinion, the major conclusion of this study is that nonconvex interparticle interactions alone can be responsible for the occurrence of periodically modulated structures when the substrate potential is convex, and that the kind of phase transitions present strongly depends on whether or not the particles experience the nonconvex part of the interaction. Some of the interesting features that we have found include both first- and second-order phase transitions, as well as sequences of transitions suggestive of a devil's-staircase[16,17] behavior. We also note the possibility of "quasicontinuous" transitions (i.e., an infinite sequence of first-order transitions) as suggested by Yokoi et al.[14] for the chiral XY model. This behavior is similar to the one found[3,5] for the ANNNI model close to the multiphase point.[3,5] We have also found sequences of "superdegenerate" points[18] in parameter space. As for the multiphase point of the ANNNI model, the ground state is infinitely degenerate at these points. However, at some of these superdegenerate points, it is seen numerically that, contrary to the multiphase point of the ANNNI model, only a finite number of phases merge. A similar behavior has been found for the chiral XY model.[14]

The organization of the paper is as follows: The models and some of their important properties are presented in Sec. II. In order to make the paper more accessible and to clarify the notation, we present in Sec. III a brief and slightly modified version (since a convex substrate potential is used instead of a periodic potential) of the powerful numerical algorithm proposed recently by Griffiths and Chou[19,20] that we have used to find the ground states of our models. The results, including phase diagrams, are presented in Sec. IV. Finally, the main results are discussed and summarized in Sec. V.

II. PRESENTATION OF THE MODELS

We consider a classical one-dimensional (1D) chain of atoms described by the Hamiltonian

$$H = \sum_{n=1}^{\infty} [V(u_n) + W(u_{n+1} - u_n)] , \qquad (2.1)$$

where u_n is the displacement of the nth particle with respect to some reference position, here assumed to be a regular one-dimensional (1D) lattice of equally spaced points. The external single-particle potential has the form

$$V(x) = \tfrac{1}{2} K x^2 \quad (K > 0) . \qquad (2.2)$$

Physically, $V(u_n)$ is the local potential experienced by a particle in the nth cell as a result of the interaction

with a background of rigid atoms. If we restrict ourselves to small deviations from symmetric equilibrium positions, $V(u_n)$ is written as in (2.2). Note that although unbounded potentials such as in (2.2) are useful for describing structural phase transitions,[21] they are not appropriate for materials where particles can jump from one unit cell to another. As usual, the ground state of (2.1) represents the equilibrium structure of a three-dimensional (3D) system of identical chains with all the transverse couplings favoring a parallel alignment of planes of atoms so that they need not be included in the Hamiltonian.

As for the ANNNI model, unbounded potentials such as (2.2) confine each particle to its cell and therefore, the average lattice distortion $\langle u_{n+1} - u_n \rangle$ must be zero in the ground state,

$$\langle u_{n+1} - u_n \rangle \equiv \lim_{N \to \infty} \left[\frac{1}{N} \sum_{n=1}^{N} (u_{n+1} - u_n) \right] = 0 . \qquad (2.3)$$

Were this not so then one would have $\langle u_{n+1} - u_n \rangle = \delta$, and the energy $E(N)$ of a chain of N atoms would increase dramatically with N,

$$E(N) \sim \sum_{n=1}^{N} V(n\delta) . \qquad (2.4)$$

The fact that $V(x)$ is convex implies (see the Appendix) that the ground state is always uniform (all the $u_n = 0$) when $W(x)$ is also a convex function. *Hence, if $V(x)$ is convex, frustration that leads to modulated ground states can only occur if $W(x)$ is nonconvex.* In order to discover which kinds of modulated ground states can occur in the presence of nonconvex interactions, we have focused our attention on two qualitatively different forms for $W(x)$:

$$W(x) = (x - \gamma)^2 - |x - \gamma| \quad (\text{model 1}) , \qquad (2.5)$$

$$W(x) = -\tfrac{1}{2}(x - \gamma)^2 + \tfrac{1}{4}(x - \gamma)^4 \quad (\text{model 2}) . \qquad (2.6)$$

Perhaps the most significant difference between these two models is the fact that the region of nonconvexity of $W(x)$ is of finite width ($|x - \gamma| < 3^{-1/2}$) in model 2, whereas it is limited to the nonanalytic point $x = \gamma$ in model 1.

Model 1 is typical of the $T = 0$ double-quadratic-well effective interparticle interaction, which arises in a 1D magnetoelastic problem[10] involving n-component classical spins, S_n, coupled to their nearest neighbors through an exchange integral which varies linearly with interparticle spacing. The exchange energy of the bonds is proportional to $-|u_{n+1} - u_n - \gamma|$ since, at $T = 0$, the classical n vectors, S_n, align themselves either ferromagnetically or antiferromagnetically with their first-nearest neighbors depending on the sign of the exchange integral between them. $-\gamma$ is the ratio of the exchange integral, J_0, to its gradient, $-J_1$, evaluated at $u_{n+1} - u_n = 0$. The first term $(x - \gamma)^2$ comes from the first-neighbor elastic interaction. At finite temperatures, it has been found[10] that the effective interaction between the u_n has the form of an analytic double-well potential if the spin-exchange interactions are 1D (more details concerning

magnetoelastic problems will be given in a later publication). In this case, model 2 serves, under certain conditions, as an approximation to this effective, temperature-dependent, interparticle interaction. More generally, (2.6) represents the first terms of a Taylor expansion of a more general nonconvex interparticle interaction as has been proposed for TlHF$_2$.[15]

It should be noted that the particular choice of the coefficients used in (2.2), (2.5), and (2.6) can always be achieved by means of an appropriate scaling of lengths and energies. Moreover, since the average lattice distortion is zero in the ground state, one could add to (2.1) the linear symmetry-breaking term $(u_{n+1} - u_n)$ without changing the ground state. However, the action of a pressure (or a tension) can be simulated, to first order, by changing the parameter γ (keeping K constant). For model 2, cubic terms can also be scaled away. If the term $\frac{1}{3}C(x - \gamma)^2$ is added to (2.6), then it can be eliminated by transforming the Hamiltonian according to

$$(K, \gamma) \rightarrow \left[\frac{K}{\xi^2}, \frac{1}{\xi} \left[\gamma + \frac{C}{3} \right] \right] ,$$

where $\xi^2 = 1 + \frac{1}{3}C^2$.

Since the Hamiltonian has the following symmetry,

$$H(\gamma, \{u_n\}) = H(-\gamma, \{-u_n\}) , \qquad (2.7)$$

it is sufficient to consider the part $\gamma \geq 0$ of the phase diagram. Moreover, Yokoi et al.[14] have shown that, for Hamiltonians of the type given by (2.1) having $V(-x) = V(x)$, a nondegenerate ground state of even period Q must have the following structure (over one period):

$$\{u_n\} = \{ -u_Q, -u_{Q-1}, \ldots ,$$
$$-u_{Q/2+1}, u_{Q/2+1}, \ldots, u_{Q-1}, u_Q \} , \qquad (2.8)$$

with all $u_n \neq 0$, whereas a nondegenerate ground state of odd period Q must have the form

$$\{u_n\} = \{ -u_Q, -u_{Q-1}, \ldots, u_{(Q+1)/2}, \ldots, u_{Q-1}, u_Q \} , \qquad (2.9)$$

with all $u_n \neq 0$ except for $u_{(Q+1)/2} = 0$. By a nondegenerate ground state we mean a ground state from which all the other ground states can be obtained through a lattice translation[14] (i.e., a ground state with trivial degeneracy). In Sec. IV, we shall see that there exist some points in the phase diagram where the ground state is (infinitely) degenerate.

In order to identify the phases, it is convenient to define a label. Perhaps the most widely used label is the winding number[1,2] defined by the value of $\langle u_{n+1} - u_n \rangle$ in the ground state. Since this quantity is always zero in our case, we need another definition. The definition for the winding number that we have found convenient for our problem is

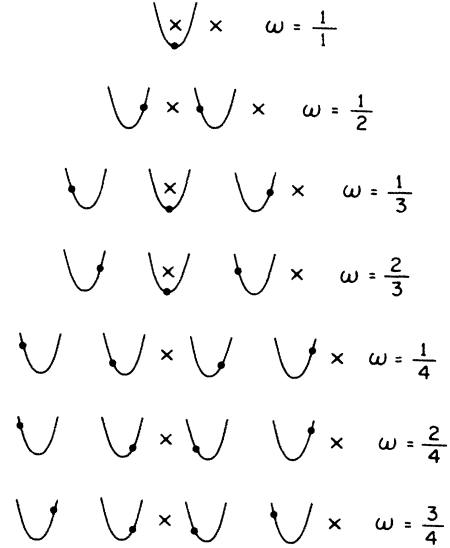$$\omega = \frac{1}{Q} \sum_{n=1}^{Q} \Theta(u_{n-1} - u_n) , \qquad (2.10)$$

FIG. 1. Examples of ground states and their winding number ω. The $\times$ denote points of reflection symmetry.

where Q is the period of the state (we restrict ourselves to states of finite periodicity), $u_0 = u_Q$ and $\Theta(x) = +1$ (if $x \geq 0$) and $\Theta(x) = 0$ (if $x < 0$). Note that the numerator and denominator are two separate integers so that, in this way, we can distinguish between the state $\omega = \frac{1}{2}$ (which has $Q = \frac{1}{2}$) and the state $\omega = \frac{2}{4}$ (which has $Q = 4$). This is illustrated in Fig. 1.

III. THE ALGORITHM OF GRIFFITHS AND CHOU

The traditional approach[1,2] to finding the ground state involves a search for the lowest-energy configuration satisfying

$$\frac{\partial H}{\partial u_n} = 0 . \qquad (3.1)$$

For the Hamiltonian (2.1), (3.1) leads to the following two dimensional (2D) map:

$$W'(u_{n+1} - u_n) = W'(u_n - u_{n-1}) + V'(u_n) , \qquad (3.2)$$

where $W'(x)$ and $V'(x)$ denote the first derivatives of $W(x)$ and $V(x)$, respectively. However, the fact that (3.2) also holds for metastable and unstable states means that the mapping problem is, in some sense, more complex than the original ground-state problem, as Aubry[2] has emphasized. Moreover, an additional and substantial difficulty arises when $W(x)$ is nonconvex, since then the 2D map (3.2) becomes multivalued.

Recently, Griffiths and Chou[19,20] have presented an algorithm that, in contrast to the traditional methods, focuses directly on the ground state and is valid for nonconvex interactions. This method is quite elegant and powerful and can be summarized as follows. Imagine that a system described by (2.1) is in its ground state. If we displace an atom from its equilibrium position, then the surrounding atoms will change their positions in or-

der to minimize the total energy. This local deformation will, in general, cost some energy and therefore, we can define a function, called the *effective potential,* which will describe this energy cost as a function of the atomic position. At site n, the effective potential $R(u_n)$, due to the presence of the atoms $i < n$, can be formally written as

$$R(u_n) \equiv \min_{i<n} \left\{ \sum_{i \le n} [W(u_i - u_{i-1}) + V(u_i) - \lambda] \right\} , \quad (3.3)$$

where λ is the (unknown) ground-state energy per particle and where the minimum must be taken over all atomic positions u_i with $i < n$. We can rewrite this equation by expressing the right-hand side (rhs) in terms of $R(u_{n-1})$ and in this manner, we obtain the following nonlinear eigenvalue equation:

$$\lambda + R(u_n) = V(u_n) + \min_{u_{n-1}} \{ W(u_n - u_{n-1}) + R(u_{n-1}) \} . $$
$$(3.4)$$

The rhs of (3.4) defines a nonlinear functional operator $\mathcal{H}$ and (3.4) can be written simply as

$$\lambda + R(u) = \mathcal{H}R(u) . \quad (3.5)$$

We can also write the effective potential $S(u_n)$ due to the presence of the atoms with $i > n$,

$$S(u_n) \equiv \min_{i>n} \left\{ \sum_{i \ge n} [W(u_{i+1} - u_i) + V(u_i) - \lambda] \right\} , \quad (3.6)$$

and the associated eigenvalue equation is

$$\lambda + S(u_n) = V(u_n) + \min_{u_{n+1}} \{ S(u_{n+1}) + W(u_{n+1} - u_n) \} . $$
$$(3.7)$$

Hence the total effective potential $F(u)$, due to all the neighboring atoms, is given by

$$F(u) = R(u) + S(u) - V(u) , \quad (3.8)$$

where $V(u)$ is subtracted in order to avoid being counted twice. When $V(-u) = V(u)$, comparison of (3.4) and (3.7) yields

$$R(u) = S(-u) , \quad (3.9)$$

and hence, in this case, all the information is contained in $R(u)$. Griffiths and Chou have showh that a continuous solution of (3.4) for $R(u)$ always exists [provided that $V(x)$ and $W(x)$ are continuous and are bounded from below] and the corresponding λ is unique (the ground-state energy must be unique).

For a given value of u_n, the value of u_{n-1} that minimizes the rhs of (3.4) defines the 1D map

$$u_{n-1} = \rho(u_n) . \quad (3.10)$$

Similarly, for a given u_n, the value of u_{n+1} that minimizes the rhs of (3.7) defines the 1D map

$$u_{n+1} = \sigma(u_n) . \quad (3.11)$$

Physically we expect that, after some initial transient be-

havior, the orbits of ρ and σ will tend to an attractor[22] which represents the ground state.[20] Hence, to generate the ground state, we only need to iterate ρ or σ once we have obtained $R(u)$ or $S(u)$.

Unfortunately, we are usually unable to find an analytic solution to (3.4) and we need to rely on numerical solutions. One way to proceed is to discretize the unit cell. We replace the continuous set of possible atomic positions by a discrete set of G points uniformly spaced on an interval D chosen sufficiently large so that the atoms are never located too near the boundaries: $u = -(D/2) + i(D/G)$ with $i = 1, 2, \ldots, G$. If $R^{(0)}(u)$ denotes the trial function $[R^{(0)}(u) = V(u)$ is a good choice], then the sequence of iterations suggested by Griffiths and Chou,

$$R^{(j+1)}(u) = \tfrac{1}{2}[\mathcal{H}R^{(j)}(u) + R^{(j)}(u)] - C_j , \quad (3.12)$$

generally converges. The constant C_j is chosen in order that the minimum value of $R^{(j+1)}(u)$ be zero. This sequence is iterated until

$$\max_u |\mathcal{H}R^{(j)}(u) - \lambda^{(j)} - R^{(j)}(u)| < \epsilon \max_u |R^{(j)}(u)| , $$
$$(3.13)$$

where the approximate ground-state energy is given by

$$\lambda^{(j)} = \min_u \{ \mathcal{H}R^{(j)}(u) \} , \quad (3.14)$$

and the final $R^{(j)}(u)$ is the approximate effective potential. We have chosen $\epsilon = 10^{-6} \rightarrow 10^{-10}$ for $G = 200 \rightarrow 3200$ points. Typically, we need about 30 iterations when $\epsilon = 10^{-6}$ and 60 iterations when $\epsilon = 10^{-10}$. However, convergence is slower near a phase transition boundary.

The major inconvenience with the discretization procedure is certainly that we cannot find any ground state with a period Q greater than the number of points G of the grid. Hence, we cannot distinguish commensurate states of period $Q \sim G$ from truly incommensurate[1,2] states, since the attractors of ρ and σ are then only periodic cycles.[22]

The amount of central-processing-unit (CPU) time increases as G^2 and becomes excessive if, for each value of u_n, a systematic search among all the possible values u_{n-1} is done to solve (3.4). For this reason, we can, at each iteration, determine an interval Δu_n (for each u_n) based on the results obtained from the previous iteration, among which the search is restrained. We can also proceed by stages: a solution obtained rapidly for $G = 25$ can then be used to generate $R^{(0)}(u)$ for $G = 50$ and so on. With these tricks, it takes about 3 s of CPU time (on an IBM 4381) to find $R(u)$ with $G = 200$ and $\epsilon = 10^{-6}$. This precision is sufficient to obtain the general aspects of a phase diagram. Finer details can be examined with larger grids of points and finer ϵ [it takes about 5 min of CPU on an IBM 4381 to obtain $R(u)$ for $G = 3200$ and $\epsilon = 10^{-10}$].

Under certain circumstances, (3.4) may have many, qualitatively different (i.e., they do not differ only by a constant) solutions $R_i(u)$. Suppose, for instance, that two phases (A and B) are separated by a first-order tran-

sition line. If $R_A(u)$ and $R_B(u)$ denote, respectively, the effective potentials of phases A and B, then any combination of the form

$$R(u) = \min_i \{R_i(u) + C_i\} , \qquad (3.15)$$

with $i = A$, B, and C_i a constant, will also be a solution along the transition line.[14,20] Due to the discretization procedure, R_A and R_B can only be determined to within a certain precision[20] $(\sim G^{-2})$. Hence, there will exist around the transition line a region of finite width where the numerical solution of (3.4) will be of the form (3.15) rather than that of a single R_i. One consequence of this is that in this region the mapping ρ has two different periodic cycles corresponding to the two phases A and B. This property turns out to be very useful in distinguishing first-order transition lines from cases where there may exist more phases between a given pair. Although this test is not absolutely rigorous, we have never been able to find other phases, upon increasing G, between two phases when we had previously observed two periodic cycles simultaneously.

IV. RESULTS

A. Effective potentials

An example of an effective potential, $R(u)$, and its associated map, ρ, is shown in Fig. 2 for model 2, for a particular choice of K and γ. Note that the first derivative of R is discontinuous at the same points where the mapping ρ is discontinuous. Also shown is the periodic cycle for the $\omega = \frac{2}{3}$ phase. Note that the local minima are not localized at the same values of u as for the periodic cycle.

It is more interesting to examine the behavior of the total effective potential $F(u)$. It is clear from Figs. 3, 4, and 5 that $F(u)$ generally has many absolute minima of equal energy. These absolute minima are localized at the possible atomic positions of the ground state. Also visible in Figs. 4 and 5 are secondary minima, higher in energy, located at metastable atomic positions. Starting from one of these secondary minima, the iteration of ρ will lead us to other secondary minima and ultimately to the ground-state periodic cycle. This sequence of atomic positions represents the left-hand part of an elementary defect which we shall call a soliton. The right-hand part of the soliton can be generated by iterating σ starting from the same secondary minimum. The soliton creation energy can be obtained by calculating the difference between $F(u)$ evaluated at the atomic positions of the defect and $F(u)$ evaluated at the atomic positions of the ground state. However, because of discretization, the result obtained in this manner may not be very precise.

The typical behavior of $F(u)$ near a second-order transition line is illustrated in Fig. 3. The transition involves a uniform $(\omega = 1/1)$ and a dimerized $(\omega = 1/2)$ phase for model 2. As the transition line is crossed, the single minimum of $F(u)$ in the uniform phase (curve 1) loses its stability (curve 2) with respect to the two minima of the dimerized phase (curve 3). Note that, because

of the absence of any secondary minimum, only the ground state is stable.

A different behavior of $F(u)$ is observed near a first-order transition line [Figs. 4(a)–4(d)]. The transition involves a dimerized and a trimerized $(\omega = 2/3)$ phase, again for model 2. Deep in the dimerized phase [Fig. 4(a)], the two absolute minima and also a secondary minimum at $u = 0$ are clearly visible. If γ is changed such that the $\omega = \frac{2}{3}$ phase is approached [Fig. 4(b)], then
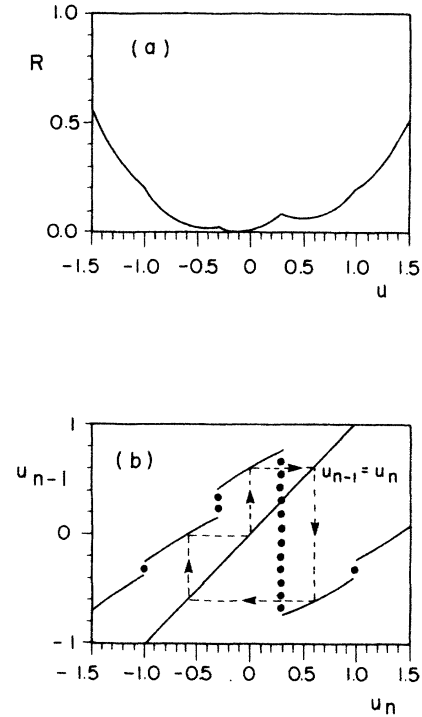

FIG. 2. (a) Effective potential $R(u)$ and (b) the associated map (solid line) $u_{n-1} = \rho(u_n)$ of model 2 for $K = 0.5$ and $\gamma = 0.33$. Also shown in (b) are the discontinuities (dotted lines), the line $u_{n-1} = u_n$, and the cycle of period 3.
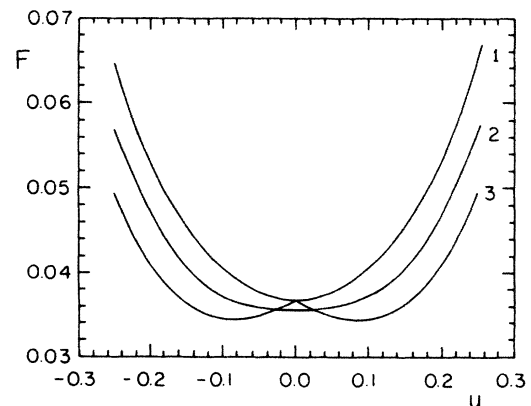

FIG. 3. Effective potential $F(u)$ in the vicinity of a second-order phase transition (model 2). $K = 3$ and $\gamma = 0.31$, 0.28868, and 0.27 for curves 1, 2, and 3, respectively.
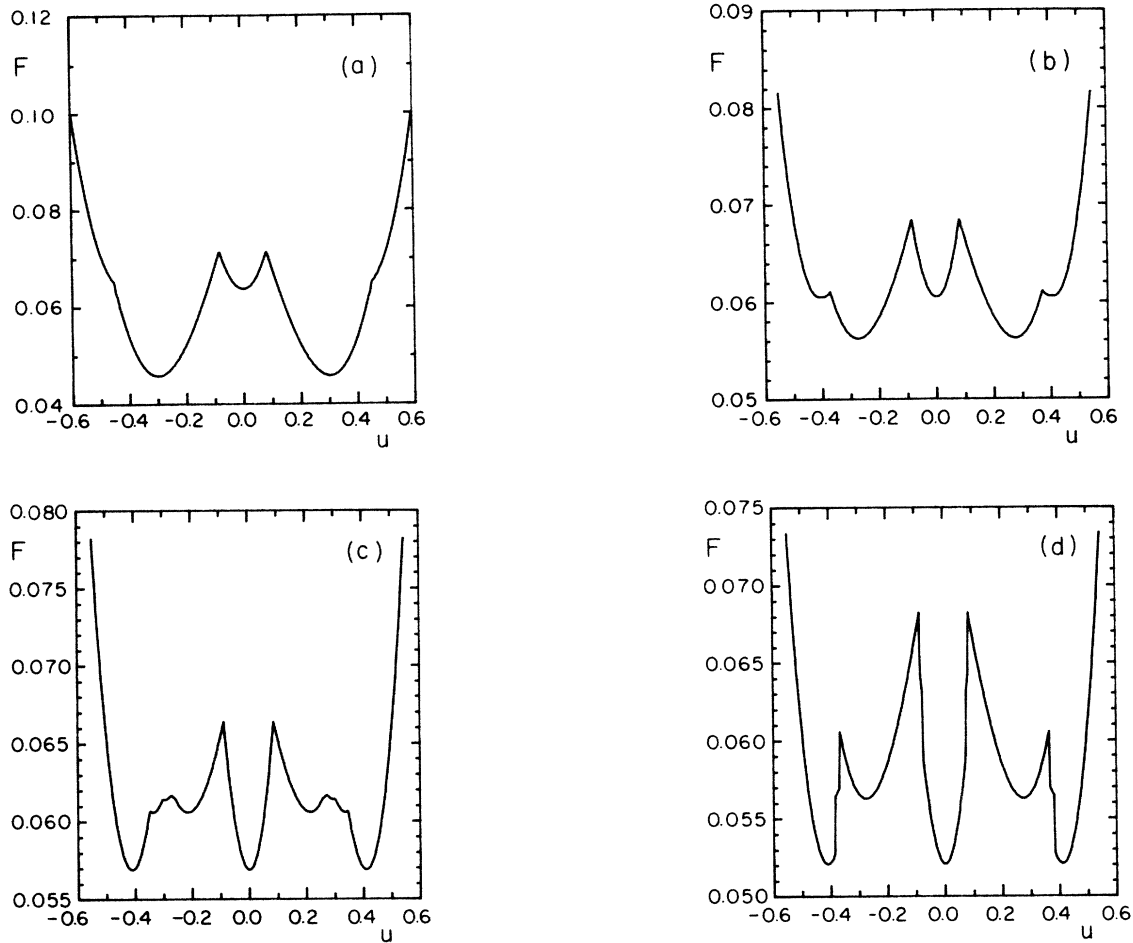
FIG. 4. Effective potential $F(u)$ in the vicinity of a first-order phase transition (model 2). (a) $K = 1.8$ and $\gamma = 0.25$, (b) 0.2875, (c) 0.2879, and (d) 0.2877.

three secondary minima, suggesting the proximity to the trimerized phase, appear. If γ is changed a little bit more [Fig. 4(c)], then we move into the trimerized phase where the three secondary minima of Fig. 4(b) become the absolute minima. Clearly, the competition between the 1/2 and 2/3 phases is reflected in the competition between the two minima of the 1/2 phase and the three minima of the 2/3 phase. The algorithm converges slowly when intermediate values of γ [values of γ between those of Figs. 4(b) and 4(c)] are used. For other intermediate values of γ (such as $\gamma = 0.2876$), the secondary and absolute minima are interchanged. In this range of γ values, the map p has two periodic cycles: one cycle of period three located at the absolute minima of Fig. 4(c) and another cycle of period two located at the absolute minima of Fig. 4(b). The iteration of p then leads us to one of these two attractors depending on the starting position.

In model 1, $F(u)$ behaves differently than in the two previous examples. Deep in the dimerized phase [Fig. 5(a)], only one secondary minimum is visible but two more secondary minima appear [Fig. 5(b)] when γ is changed slightly, suggesting the proximity of a trimer-

ized phase. Note, however, that two other secondary minima, suggesting the proximity of a period-5 phase, appear [Fig. 5(c)] if γ is changed a bit more. As γ is varied further [Fig. 5(d)], other secondary minima appear, suggesting phases of even higher periodicities. Indeed, if $\gamma = 0.0895$ we find a phase with $\omega = 6/11$. Nowhere in model 1 have we been able to find simultaneously two different periodic cycles and it appears that $F(u)$ possess an infinity of minima, infinitely closely spaced, between the dimerized and trimerized phases. Of course, this statement cannot be numerically verified with absolute certainty. It is clear, however, that it is not a second-order transition where a phase loses its stability at the expense of another phase and also that it is probably not a first-order transition since simultaneous cycles have not been observed. In fact we believe that it is a compromise between a first-order and second-order transition: a devil's staircase.[16,17]

B. Phase diagram for model 1

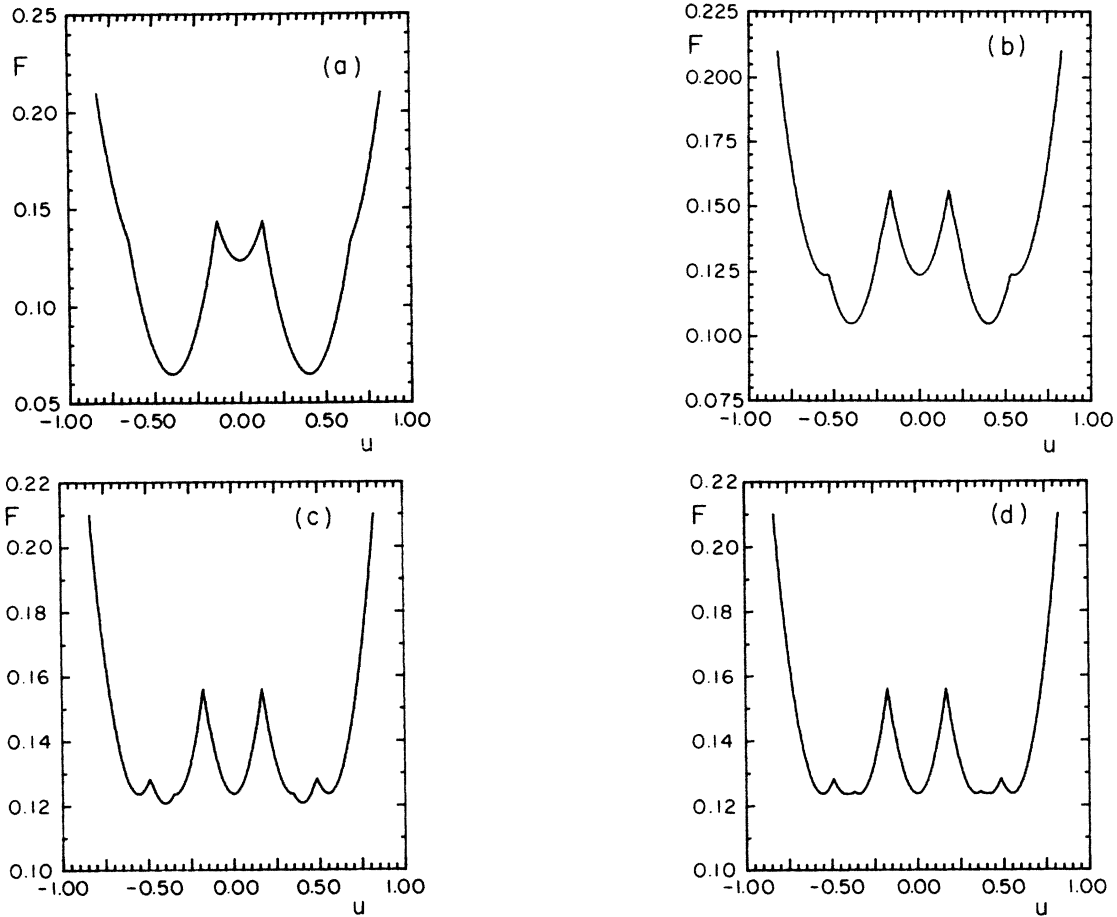Figure 6 presents the phase diagram for model 1 obtained by solving (3.4) with $G = 200$ points. Only phases

FIG. 5. Effective potential $F(u)$ in the 1/2 phase of model 1 near its phase boundary . (a) $K = 2$ and $\gamma' = 0.06$, (b) 0.08, (c) 0.088, and (d) 0.0894.

with a period $Q \leq 5$ are shown. We have used the parameters

$$\alpha \equiv (1 + K/4)^{-1} . \tag{4.1a}$$

$$\gamma' \equiv \gamma/\alpha . \tag{4.1b}$$
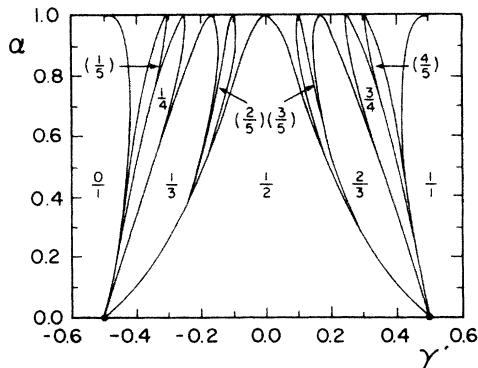
Note that, because of the symmetry properties of the

FIG. 6. Phase diagram for model 1. The numbers are values of the winding number ω. The unlabeled regions contain additional commensurate phases.

model, namely that $V(x) = V(-x)$, the P/Q phase becomes the $(Q-P)/Q$ phase when $\gamma \to -\gamma$. At $K \to 0+$, the P/Q phase tends towards $\gamma = (2P - Q)/2Q$. This last result can be obtained by searching for the value of γ that minimizes the Hamiltonian when $K = 0$ and $\omega = P/Q$.

If we recall that $-\gamma$ is the ratio of the exchange integral, J_0, to its gradient, $-J_1$, evaluated at $u_{n+1} - u_n = 0$, then the fraction, ω_γ, of antiferromagnetic bonds, for a phase of period Q, is

$$\omega_\gamma = \frac{1}{Q} \sum_{n=1}^{Q} \Theta(u_{n-1} - u_n + \gamma) . \tag{4.2}$$

We find that $\omega_\gamma = \omega$ everywhere in the phase diagram except in the uniform phase, where $\omega = 1/1$, whereas $\omega_\gamma = 1/1$ for $\gamma > 0$ and $\omega_\gamma = 0/1$ for $\gamma < 0$, as shown in Fig. 6. This result suggests that each individual bond can only distort discontinuously through an inversion of its exchange integral.

In addition, Ishimura[23] has solved the same $T = 0$ magnetoelastic problem (for the Ising case only) with the effective spin Hamiltonian obtained by a canonical transformation. Using the method of Bak and Bruinsma,[24] Ishimura has obtained a devil's staircase for $\omega_\gamma(\gamma)$.

Note the similarity of Fig. 6 with Ishimura's phase diagram. Since the effective lattice Hamiltonian (i.e., model 1) is the same for all n-vector models, Ishimura's results should be valid for any n-vector model.

We find that our results are consistent with a devil's-staircase behavior. Indeed, we have always been able to find a phase $(P+Q)/(R+S)$ between any two given phases P/Q and R/S if a sufficiently fine grid of points is used to solve (3.4) (we have used grids up to $G=3200$ points). Also, we have never been able to find simultaneously two periodic cycles as in the case of first-order transitions. Moreover, it is easy to show that any configuration $\{u_i\}$ satisfying (3.1) is linearly stable against small perturbations. Indeed, if $\{u_i+\epsilon_i\}$ denotes a state slightly perturbed from $\{u_i\}$, then the linearized equations of motion

$$-m\frac{d^2}{dt^2}\epsilon_i = V''(u_i)\epsilon_i + W''(u_{i+1}-u_i)(\epsilon_i-\epsilon_{i+1})$$

$$+ W''(u_j-u_{j-1})(\epsilon_j-\epsilon_{j-1}) \ , \qquad (4.3)$$

with $V''=K$, $W''=2$, and m the atomic mass, are those of a harmonic chain in which each particle is confined to a parabolic potential. Since all the frequencies of (4.3) are strictly positive, all configurations satisfying (3.1) are stable, and therefore any phase transition of model 1 should be accompanied by hysteresis effects. These results are all consistent with a complete devil's-staircase behavior (recalling Aubry's definition[17] of a devil's staircase) and therefore incommensurate ground states should occur in this model only with zero measure in parameter space.

Finally, it is worth mentioning that as $\alpha\rightarrow0$, $K\rightarrow\infty$ and the first-neighbor elastic interactions become negligible relative to the curvature of the external potential, so that we recover the magnetoelastic model of De Simone, Stratt, and Tobochnick,[25] which is identical to the ANNNI model. Thus the two multiphase points of Fig. 6 are those of the ANNNI model at $T=0$.

C. Phase diagram for model 2

The phase diagram for model 2 is shown in Fig. 7. As mentioned in Sec. II, the phase P/Q for $\gamma>0$ becomes the phase $(Q-P)/Q$ when $\gamma\rightarrow-\gamma$. At $K\rightarrow0+$, the P/Q phase tends towards $\gamma=(2P-Q)/Q$. Note that, in contrast with model 1, there exists a critical value of $K(K=4)$ above which the ground state is always uniform.

For the following analysis it is desirable to introduce the notation of Ref. 14. A phase is called "nonconvex" if at least one pair of atoms uses the nonconvex part of $W(x)$; otherwise it is called "convex." Some phases (the 3/5 phase, for example) are "convex" everywhere, others (the 2/4 phase, for example) are "nonconvex" everywhere. Most of the phases, however, are both "convex" and "nonconvex" in different regions of the phase diagram. A separation line, indicated by a dashed line in Fig. 7, separates the "nonconvex" region from the "convex" region of the same phase. Note that only "convex"
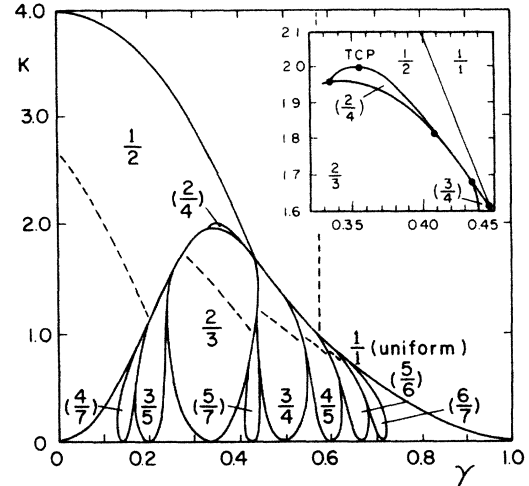

FIG. 7. Phase diagram for model 2. The numbers are values of the winding number ω. The unlabeled regions contain additional commensurate phases. The dashed lines are separation lines defined in the text. Inset: TCP indicates a tricritical point and the other points are triple points.

phases are present in model 1, since atoms are always unstable at the single nonconvex point, $x=\gamma$, of $W(x)$. In model 2, however, large portions of the phase diagram are filled with "nonconvex" phases which are located above (to the left of, for the 1/1 phase) the separation lines.

Although there is no phase transition when these separation lines are crossed, we expect (and find) that the type of transition between any two given phases strongly depends on the convexity of the phases on either side of the transition line. Indeed, Yokoi et al.[14] have shown recently that the interaction between solitons of a given commensurate phase is generally repulsive for "convex" phases but oscillatory for "nonconvex" phases. In addition, it is now well known[1,2,7,11] that the transition must be continuous (i.e., a devil's staircase) when the soliton interaction is always repulsive and that it occurs when the soliton creation energy vanishes. The solitons then condense with zero density at the transition line. If, however, there is a distance for which the interaction between solitons is attractive, then the transition must be discontinuous[11] (i.e., of first order) and must take place before the soliton creation energy vanishes. In this case, solitons condense with a finite density.

The same numerical evidence that supports the existence of a devil's staircase in model 1 is also present in model 2 for transitions between "convex" phases. For example, between the 3/5 phase (which is "convex" everywhere) and the "convex" 2/3 phase, we are always able to find (with a sufficiently fine grid of points) an intervening phase $(P+Q)/(R+S)$ between any two given phases P/Q and R/S, all of which are "convex." Furthermore, as can be seen directly from (4.3), "convex" phases are structurally stable and, therefore, hysteresis effects should be present. Hence, in this region of the phase diagram, our results are consistent with a com-

plete devil's-staircase behavior. Although it is impossible to distinguish high-order commensurate states from truly incommensurate states when using this numerical algorithm, we believe that incommensurate ground states can only occur in this model with zero measure in parameter space because, in order that hysteresis effects be absent, it is necessary (since V is convex) that some of the particles experience the nonconvex part of W. On the other hand, between "nonconvex" phases we have observed two different kinds of behavior. Firstly, we have found second-order phase transitions between the "nonconvex" 1/1 and 1/2 phases where the uniform state is unstable against dimerization along the parabola $K +4(3\gamma^2 -1)=0$ and between the phase 1/2 and the (everywhere "nonconvex") 2/4 phase to the left of the tricritical point (TCP) (the transition is first order to the right of the TCP). Secondly, first-order transitions and triple points have been found in several places in the phase diagram. Examples of triple points are shown in the inset of Fig. 7. It is straightforward to show, by finding the state that has the lowest energy among states of period lower than 5, that the transitions between the phases 1/2 and 2/3, 1/2 and 3/4, 2/4 and 2/3, and 2/3 and 3/4 are all first order.

The presence of the "nonconvex" 2/4 phase is another feature of model 2 that differs from model 1. Other "nonconvex" phases where the numerator and the denominator have a common divisor are also found in this model. For example, note the presence of the 4/6 phase in a narrow region of Fig. 8. This phase springs from the point SDU$_2$ where the 5/6 phase disappears. The position of the atoms in the 4/5, 5/6, and 4/6 phases near the point SDU$_2$ is illustrated in Fig. 9. The amplitudes of atomic displacements u_1, u_2, and ϵ are all, by convention, positive and $\epsilon \to 0$. The amplitudes u_1 and u_2 are the same for these three phases. Note that the 4/6 and 5/6 phases are identical when $\epsilon = 0$. In this case, we can consider the group of atoms $\{-u_2, -u_1, u_1, u_2\}$ as a soliton of the uniform phase. These solitons are noninteracting, since they are separated by a sufficiently large number of atoms (two for a Hamiltonian where the range of interaction is limited to
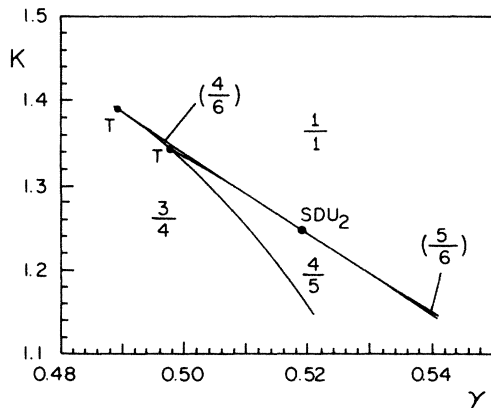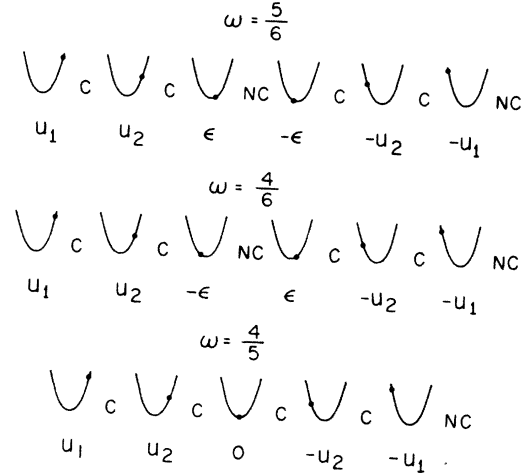

FIG. 9. Structure of the ground states near the point SDU$_2$. NC and C denote nonconvex and convex bonds, respectively.

first neighbors) at positions corresponding to the uniform phase. Hence, we have infinite degeneracy when $\epsilon = 0$ since, starting from this state of period 6, we can build an infinite number of other states of the same energy by separating these solitons by an arbitrary number (larger than two) of atoms located at $u = 0$. If this state is the ground state at SDU$_2$, then SDU$_2$ would be a superdegenerate point where the ground state is infinitely degenerate and where the third law of thermodynamics is violated.

D. Superdegenerate points

By using only the numerical algorithm of Griffiths and Chou we are unable to definitely verify that SDU$_2$ is a superdegenerate point. Therefore, we take a different approach which involves finding the locus of points (K, γ) where the 2D map (3.2) gives a phase of period 6 with two consecutive atoms located at $u = 0$. We then obtain the following three equations:

$$\phi(u_2 + \gamma) = \phi(\gamma) , \tag{4.4a}$$

$$\phi(u_1 - u_2 + \gamma) - Ku_2 = \phi(\gamma) , \tag{4.4b}$$

$$\phi(\gamma - 2u_1) - Ku_1 = \phi(u_1 - u_2 + \gamma) , \tag{4.4c}$$

where the amplitudes u_1 and u_2 are defined in Fig. 9 and the function $\phi(x)$ is obtained from W':

$$\phi(x) = x^3 - x . \tag{4.5}$$

Note that we have used $\phi(-x) = -\phi(x)$. Equation (4.4a) is obtained from (3.2) when $u_{n-1} = u_n = 0$ and $u_{n+1} = -u_2$. It is important to note that in this case $u_{n+1} = 0$ is also a solution of (3.2). In addition, a solution of (4.4a) with $u_2 > 0$ exists only if $\gamma < 1/\sqrt{3}$ (i.e., to the left of the separation line of the uniform phase). Equation (4.4b), obtained from (3.2) when $u_{n-1} = 0$, $u_n = -u_2$, and $u_{n+1} = -u_1$, has a solution only if $u_1 > 2u_2$ or $u_1 < u_2$; however, this last possibility has to be rejected since this bond is convex. Equation (4.4c) is

FIG. 8. Phase diagram of model 2 around the point SDU$_2$. T denotes a triple point.

obtained from (3.2) when $u_{n-1} = -u_2$, $u_n = -u_1$, and $u_{n+1} = u_1$. The three remaining equations that can be obtained from (3.2) are identical to (4.4).

The solution of (4.4) defines a line $K(\gamma)$, which is plotted in Fig. 10(a) and along which the solitons are noninteracting. The point on this line [Fig. 10(b)] where the phase of period 6 (with two consecutive atoms at $u = 0$) has the same energy as the uniform phase, is the point where the phases 4/5, 5/6, 4/6, 1/1, and infinitely many other phases have the same energy. We conclude that this point will be a superdegenerate point if at this point the algorithm of Griffiths and Chou gives the phase 1/1 or the phase 4/5 [with the atomic positions consistent with those obtained from (4.4)]. However, if the algo-

rithm finds another phase P/Q, then the ground state will be this nondegenerate state P/Q at this point. We have obtained the 1/1 phase and hence we conclude that SDU_2 is a superdegenerate point. However, in contrast with the multiphase points of model 1, there are only four phases springing from this point. Indeed, only first-order transitions are observed between the phases shown in Fig. 8.

We can use this technique to see if other superdegenerate points exist along the boundary of the 1/1 phase. Generally, the line $K(\gamma)$, along which the phase of period Q (Q is an even number) has two consecutive atoms at $u = 0$, is obtained by solving the following system of equations [obtained from (3.2)]:

$$
\begin{aligned}
&\phi(u_M + \gamma) = \phi(\gamma), \\
&\phi(u_{M-1} - u_M + \gamma) - K u_M = \phi(u_M + \gamma), \\
&\phi(u_{M-2} - u_{M-1} + \gamma) - K u_{M-1} = \phi(u_{M-1} - u_M + \gamma), \\
&\phi(u_{M-3} - u_{M-2} + \gamma) - K u_{M-2} = \phi(u_{M-2} - u_{M-1} + \gamma), \\
&\vdots, \\
&\phi(u_1 - u_2 + \gamma) - K u_2 = \phi(u_2 - u_3 + \gamma), \\
&\phi(\gamma - 2u_1) - K u_1 = \phi(u_1 - u_2 + \gamma),
\end{aligned}
\qquad M - 1 \text{ equations}
\qquad (4.6)
$$

where the u_i are the amplitudes of the atomic displacements and $M = (Q - 2)/2$. By definition, the point SDU_M is the point on the line $K(\gamma)$ where the phase of period Q, with two consecutive atoms at $u = 0$, has the same energy as the uniform phase. Equations (4.4) are Eqs. (4.6) when $M = 2$. The first equation of (4.6) indicates that all the points SDU_M are located to the left of the separation line of the uniform phase (i.e., for $\gamma < 1\sqrt{3}$). The coordinates (K, γ) of the points SDU_M

(for $M = 1$, 2, 3, 4, and 5) and the amplitudes u_i, obtained by solving (4.6), are listed in Table I. Note that SDU_1 is the only such point which does not occur as a superdegenerate point in the phase diagram, since the algorithm of Griffiths and Chou gives the 1/2 phase at that point. Indeed, as already mentioned in Sec. IV C, only triple points are found between the phases 2/4, 3/4, 2/3, and 1/1 (see inset of Fig. 7) when a systematic search for the states of lowest energy among states of period lower than 5 is made. However, this method becomes extremely cumbersome when we increase the maximum periodicity over which the ground state is searched. This is why we use the Griffiths and Chou algorithm as the final test to see whether or not an SDU_M point is in fact a superdegenerate point.

From the above investigation, we propose Fig. 11 as a schematic representation of the phase diagram along the uniform phase boundary. We have been able to confirm, by observing simultaneously two periodic cycles, that the transitions around SDU_2 and SDU_3 are all first order and we believe that it is also the case for the transitions around the other SDU_M points, since all the phases are "nonconvex" in these regions. It seems that the SDU_M points are all superdegenerate points and accumulate on the point SDU_∞ located on the line $\gamma = 1\sqrt{3}$. If this is the case, then all the phases $(Q - 1)/Q$ should converge in this region near SDU_∞. A similar behavior was found by Yokoi et al.[14] for the chiral XY model.

We think that superdegenerate points are found in many regions of the phase diagram. Figure 12 shows a small portion of the phase diagram near the dimerized phase. The 4/7 phase seems to disappear at the point
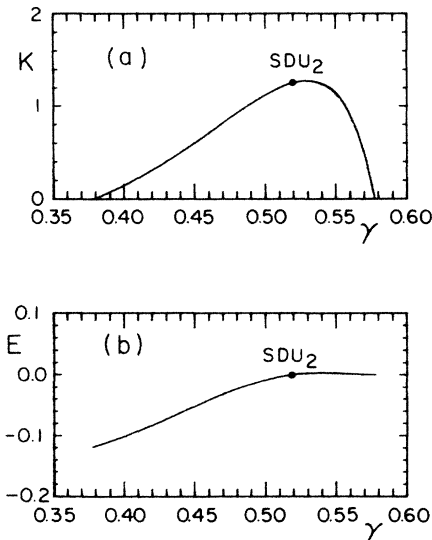
FIG. 10. (a) Curve $K(\gamma)$ obtained by solving (4.4), and (b) the energy $E(\gamma)$ of this phase of period 6 minus the energy of the uniform phase [on the line $K(\gamma)$].

TABLE I. Location of the points SDU_M. The uncertainty is one in the last digit. In the column labeled SD we have indicated whether or not the point SDU_M is a superdegenerate point.

Point	Coordinate K	Coordinate γ	Amplitudes	SD
SDU_1	1, 714 285 714	0, 428 571 429	$u_1 = 0$, 285 714 286	no
SDU_2	1, 248 262 049	0, 518 876 524	$u_1 = 0$, 446 409 274	yes
			$u_2 = 0$, 115 035 854	
SDU_3	1, 051 996 809	0, 562 914 104	$u_1 = 0$, 506 487 626	yes
			$u_2 = 0$, 171 454 697	
			$u_3 = 0$, 028 752 994	
SDU_4	0, 995 923 167	0, 576 203 682	$u_1 = 0$, 523 851 301	yes
			$u_2 = 0$, 189 118 264	
			$u_3 = 0$, 039 391 936	
			$u_4 = 0$, 002 292 416	
SDU_5	0, 991 174 197	0, 577 344 696	$u_1 = 0$, 525 328 629	yes
			$u_2 = 0$, 190 649 177	
			$u_3 = 0$, 040 347 348	
			$u_4 = 0$, 002 540 394	
			$u_5 = 0$, 000 011 146	

SDD_1. The positions of the atoms in the 4/7 phase, slightly over and slightly under the point SDD_1 are presented in Fig. 13. The amplitude, a, of the dimerized phase is simply found by searching for the value of a that minimizes H when $u_n = (-1)^n a$:

$$a = \tfrac{1}{4}(4 - K - 12\gamma^2)^{1/2} . \tag{4.7}$$

From Fig. 13, we see that the sequence $\{u_1, 0, -u_1\}$ forms a soliton of the dimerized phase when $\epsilon = 0$. These solitons are noninteracting, since they are separated by a sufficiently large number of atoms (four) in the dimerized phase. The line $K(\gamma)$, on which the 4/7 phase has four consecutive atoms in the dimerized phase, is obtained by solving the system of equations [obtained from (3.2)]

$$\phi(u_1 + a - \gamma) = \phi(2a - \gamma) , \tag{4.8a}$$

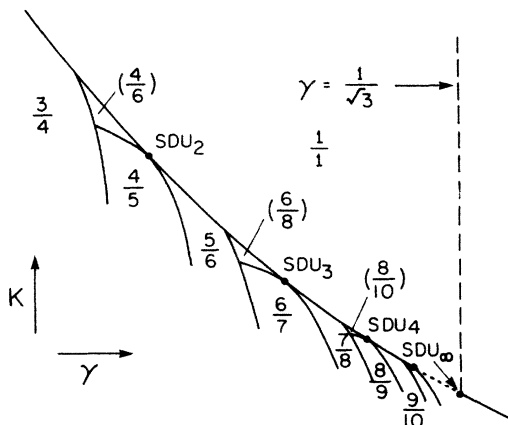$$\phi(-u_1 - \gamma) - Ku_1 = \phi(u_1 + a - \gamma) . \tag{4.8b}$$

We define the point SDD_1 as the point on the line $K(\gamma)$ where the energy of this 4/7 phase is the same as the energy of the 1/2 phase. At this point, the phases 1/2, 4/7, 3/5, and also infinitely many other states (obtained by separating the solitons by an arbitrary number, greater than four, of atoms) have the same energy. We will conclude that this point is a superdegenerate point if the Griffiths and Chou algorithm gives, at this point, the 1/2 phase or the 3/5 phase [with the atomic positions in accordance with those obtained from (4.7) and (4.8)]. We have obtained the 3/5 phase with the correct atomic positions and we conclude that SDD_1 is in fact a superdegenerate point.

We have found other SDD_M points between the phases 1/2, $(M+2)/(2M+3)$, and $(M+3)/(2M+5)$, where M is an odd integer $(M = 1, 3, 5, \ldots,)$. The phase $(M+3)/(2M+5)$, formed by a regular array of noninteracting solitons of the dimerized phase, exists on the line $K(\gamma)$ obtained by solving the system of equations [from (3.2)]
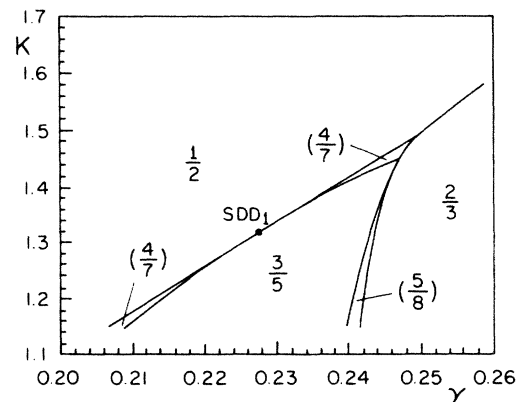

FIG. 11. Structure of the phase diagram of model 2 (schematic) near the 1/1 phase boundary.

FIG. 12. Phase diagram of model 2 near the point SDD_1.

$$\phi(u_1 + a - \gamma) = \phi(2a - \gamma) \, ,$$

$$\phi(-u_2 - u_1 - \gamma) - Ku_1 = \phi(u_1 + a - \gamma) \, ,$$

$$\phi(u_3 + u_2 - \gamma) + Ku_2 = \phi(-u_2 - u_1 - \gamma) \, ,$$

$$\vdots \, ,$$

$$\phi(u_M + u_{M-1} - \gamma) + Ku_{M-1} = \phi(-u_{M-1} - u_{M-2} - \gamma) \, ,$$

$$\phi(-u_M - \gamma) - Ku_M = \phi(u_M + u_{M-1} - \gamma) \, .$$

$M - 1$ equations   (4.9)

The general structure of the phase $(M+3)/(2M+5)$ on the line $K(\gamma)$ and the definition of the amplitudes u_i used to write (4.9) are found in Fig. 14. The point SDD_M is defined as the point on $K(\gamma)$ where the energy of the phase $(M+3)/(2M+5)$ is identical to that of the $1/2$ phase. Note that the first equation of (4.9) indicates that all the SDD_M points are located above the separation line of the $1/2$ phase (i.e., for $2a - \gamma < 1/\sqrt{3}$). The coordinates (K,γ) of the SDD_M points (for $M = 1, 3, 5,$ and 7) and the amplitudes are listed in Table II. Using the criteria mentioned above, we have found that they are all superdegenerate points.

From these results, we propose Fig. 15 as a schematic representation of the phase diagram along the boundary of the dimerized phase. However, in contrast to the behavior found near the boundary of the uniform phase, the phase transitions surrounding the SDD_M points are necessarily of first order, since we have not been able to observe simultaneously two periodic cycles between any of these phases. Hence, other phases may exist between the $(M+2)/(2M+3)$ and $(M+3)/(2M+5)$ phases. However, we have not been able to find them. In addition, it is important to mention that, while the $(M+3)/(2M+5)$ phases are "nonconvex" around the

SDD_M points, the $(M+2)/(2M+3)$ phases are "convex" everywhere. Following Yokoi et al.[14] and Villain and Gordon,[11] this suggests a continuous transition when leaving the $(M+2)/(2M+3)$ phases but a discontinuous transition when leaving the $(M+3)/(2M+5)$ phases and hence, quasicontinuous transitions.[14]

E. Quasicontinuous transitions

The region of the phase diagram where the possibility of a quasicontinuous transition is most apparent is shown in Fig. 16. In this region, the $2/3$ phase is "convex", whereas the $1/2$ and the $4/7$ phases are "nonconvex." Also visible in Fig. 16 is the "nonconvex" $6/10$ phase separated from the $4/7$ phase by a first-order transition. In between the $6/10$ and the $2/3$ phases, we have also found the "nonconvex" $8/13$ phase separated from the $6/10$ phase by a first-order transition. It seems reasonable that this process continues to infinity. In that case, the resulting phase diagram would be as shown in Fig. 17, every transition being of first order except for the last devil's-staircase step[3] located on the boundary of the $2/3$ phase. This seems to be an elegant compromise for transitions between "convex" and "nonconvex" phases following from the fact that we expect[11,14] a discontinuous transition when leaving a "nonconvex" phase but a continuous transition when leaving a "convex" phase.

V. CONCLUSION

In this paper we have presented a detailed (but certainly not complete) analysis of 1D models where frustration results from the presence of nonconvex interparticle interactions. The resulting phase diagrams turn out to be qualitatively different depending on whether or not the particles in the ground state experience the nonconvex part of the interaction. When the particles experi-
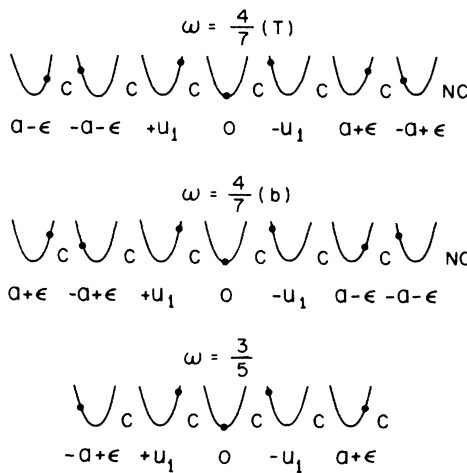
FIG. 13. Structure of the ground states near the point SDD_1. (T) denotes the superior part of the $4/7$ phase and (B) the inferior part of the $4/7$ phase relative to the location of the point SDD_1. NC and C denote nonconvex and convex bonds, respectively.
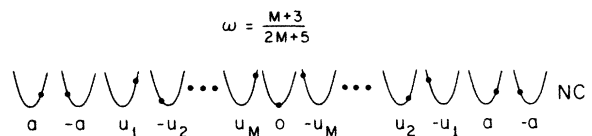
FIG. 14. Structure of the ground state of period $2M + 5$ at the point SDD_M. The only nonconvex bond is identified by NC.

TABLE II. Location of the points SDD_M. The uncertainty is one in the last digit. In the column labeled SD we have indicated whether or not the point SDD_M is a superdegenerate point.

Point	Coordinate K	Coordinate γ	Amplitudes	SD
SDD_1	1, 318 992 878	0, 227 251 518	$u_1 = 0,\ 528\,268\,172$	yes
SDD_3	1, 118 885 289	0, 203 000 781	$u_1 = 0,\ 402\,018\,510$	yes
			$u_2 = 0,\ 360\,730\,956$	
			$u_3 = 0,\ 576\,200\,170$	
SDD_5	1, 097 792 958	0, 200 515 065	$u_1 = 0,\ 389\,069\,189$	yes
			$u_2 = 0,\ 388\,598\,313$	
			$u_3 = 0,\ 406\,457\,753$	
			$u_4 = 0,\ 360\,550\,609$	
			$u_5 = 0,\ 581\,187\,194$	
SDD_7	1, 097 546 560	0, 200 486 074	$u_1 = 0,\ 388\,918\,188$	yes
			$u_2 = 0,\ 388\,918\,134$	
			$u_3 = 0,\ 389\,102\,495$	
			$u_4 = 0,\ 388\,625\,680$	
			$u_5 = 0,\ 406\,507\,745$	
			$u_6 = 0,\ 360\,551\,082$	
			$u_7 = 0,\ 581\,234\,050$	

ence only the convex part of the interaction potential, as for model 1, only phases where the winding number is uniquely defined (i.e., when the numerator and denominator do not have a common divisor) are found, and the transitions among these phases are suggestive of a complete devil's-staircase behavior. When some of the particles in the ground state experience the nonconvex part of the interaction potential, phases where the winding number is not uniquely defined (the 2/4 phase, for example) are found in the phase diagram. In this case, both first- and second-order phase transitions and possibly quasicontinuous transitions are found. Also of interest is the existence of sequences of superdegenerate points where the system has residual entropy and violates the

third law of thermodynamics. At these points, we have shown that the ground state consists of noninteracting solitons of zero energy.

Finally, it is worth mentioning that the phase diagram of model 2 is quite similar to that obtained by Yokoi et al.[14] for the chiral XY model in a magnetic field. However, important differences occur at low fields, where their phase diagram becomes very similar to that of the Frenkel-Kontorova model. Indeed, the width of the main commensurate phases for small K are substantially larger for model 2 than for the chiral XY model at low fields. This fact supports our conjecture that, in contrast to the XY model, incommensurate ground states can occur in model 2 only with zero measure in parameter space. Also of importance is the fact that the phase
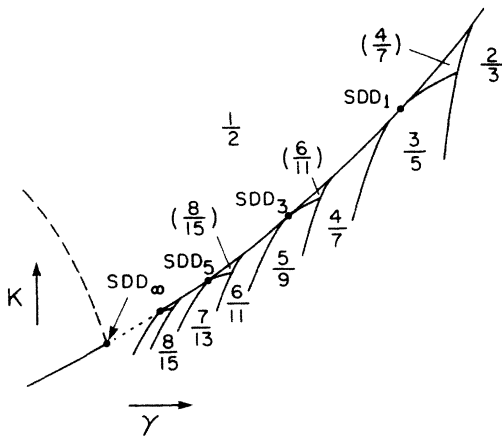

FIG. 15. Structure of the phase diagram of model 2 (schematic) near the boundary of the 1/2 phase.
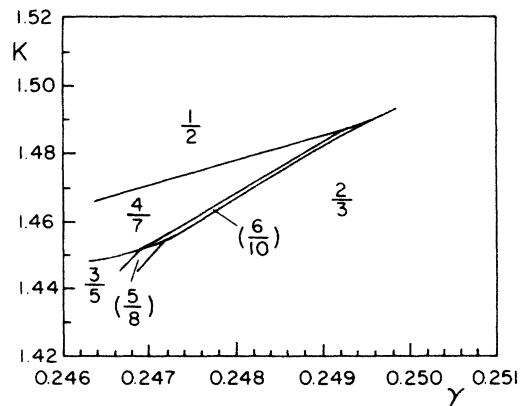

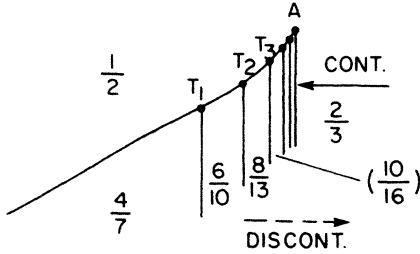FIG. 16. Phase diagram of model 2 near the 4/7 and 2/3 phases.

FIG. 17. Probable structure of the phase diagram of model 2 (schematic) in between the 4/7 and 2/3 phases. The T_i's denote triple points that accumulate at point A.

diagram of Ref. 14 reveals the existence of a superdegenerate point at the crossings of the 2/4, 3/4, 2/3, 1/2, and 1/1 phases, whereas only triple points are found for model 2 in this region. In a later publication (on magnetoelastic problems) we will show that this superdegenerate point can "split" into triple points exactly when the 1/2 phase boundary meets the superdegenerate point and that the situation encountered in the XY model corresponds to a marginal case.

ACKNOWLEDGMENTS

APPENDIX

We now proceed to show that there is only one (unmodulated) ground state when both $W(x)$ and $V(x)$ are convex (for any γ). To demonstrate this, we need to prove that the energy $E_{\text{mod}}(N)$ of a sequence of N atoms in any modulated state of period N (with N an arbitrary integer) is always larger than the enregy $E_{\text{uni}}(N)$ of these same N atoms in the uniform state (all $u_n = 0$) when both $V(x)$ and $W(x)$ are convex. We have

$$E_{\text{mod}}(N) = \sum_{n=1}^{N} [V(u_n) + W(u_{n+1} - u_n)]$$

$$\text{with } (u_{N+1} = u_1) , \qquad \text{(A1)}$$

$$E_{\text{uni}}(N) = \sum_{n=1}^{N} [V(0) + W(0)] . \qquad \text{(A2)}$$

Recall that by definition of $V(x)$ and u_n, the minimum of $V(x)$ is at $x = 0$. Hence, for at least one nonzero u_n,

$$\sum_{n=1}^{N} V(u_n) > NV(0) . \qquad \text{(A3)}$$

Moreover, since $V(x)$ is convex (and therefore unbounded), the $average$ lattice spacing $\langle u_{n+1} - u_n \rangle$ has to be zero in the ground state. Hence, among states of finite period N, we need only consider those that satisfy the constraint

$$\delta_N \equiv \sum_{n=1}^{N} v_n = 0 \quad (v_n \equiv u_{n+1} - u_n) , \qquad \text{(A4)}$$

since a state of period N with nonzero δ_N has an energy that increases as

$$\sum_{j=1}^{M} V(j\delta_N) ,$$

where M is the number of segments of N atoms. This rate of increase, as a function of M, is extremely large when $V(x)$ is convex but not when $V(x)$ is nonconvex and bounded as in the Frenkel-Kontorova model. In order to show that $E_{\text{mod}}(N) > E_{\text{uni}}(N)$ for $\delta_N = 0$, we only need to prove that

$$\sum_{n=1}^{N} [W(v_n) - W(0)] > 0 \quad \text{for } \delta_N = 0 . \qquad \text{(A5)}$$

Recall that a convex function $f(x)$ has, by definition, a first derivative that increases monotonously at every x. Construct the following positive convex function $G(v_n)$:

$$G(v_n) \equiv W(v_n) - [W(0) - v_n W'(0)] ,$$

where $W'(0)$ denotes the first derivative of $W(x)$ at $x = 0$. Then when $\delta_N = 0$, (A5) can be written as

$$\sum_{n=1}^{N} G(v_n) > 0 , \qquad \text{(A6)}$$

which is always satisfied for at least one nonzero v_n, since $G(x)$ is positive. This completes the proof.

*Present address: Institut für Festkörperforschung der Kernforschungsanlage Jülich G.m.b.H., Postfach 1913, D-5170 Jülich, West Germany.

[1]For a review, see P. Bak, Rep. Prog. Phys. **45**, 587 (1982).

[2]For a clear and rigorous presentation, see S. Aubry, in *Structures et Instabilités*, edited by C. Godrèche (Les éditions de Physique, Paris, 1987), pp. 73–192.

[3]M. E. Fisher and W. Selke, Phys. Rev. Lett. **44**, 1502 (1980).

[4]P. Bak and J. von Boehm, Phys. Rev. B **21**, 5297 (1980).

[5]W. Selke and P. M. Duxbury, Z. Phys. B **57**, 49 (1984).

[6]T. De Simone and R. M. Stratt, Phys. Rev. B **32**, 1537 (1985).

[7]F. Axel and S. Aubry, J. Phys. C **14**, 5433 (1981).

[8]T. Janssen and J. A. Tjon, Phys. Rev. B **25**, 3767 (1982).

[9]M. Marchand, K. H. Hood, and A. Caillé, Phys. Rev. Lett. **58**, 1660 (1987).

[10]M. Marchand, A. Caillé, and R. Pépin, Phys. Rev. B **34**, 4710 (1986).

[11]J. Villain and M. B. Gordon, J. Phys. C **13**, 3117 (1980).

[12]S. Aubry, K. Fesser, and A. R. Bishop, Ferroelectrics **66**, 151 (1986).

[13]A. Banerjea and P. L. Taylor, Phys. Rev. B **30**, 6489 (1984).

[14]C. S. O. Yokoi, L. Tang, and W. Chou, Phys. Rev. B (to be published).

[15]E. V. Kholopov, Solid State Commun. **47**, 187 (1983).

[16]B. Mandelbrot, *Fractals: Form, Chance, and Dimension* (Freeman, San Francisco, 1977).

[17]S. Aubry, J. Phys. C **16**, 2497 (1983).

[18]J. L. Lebowitz, M. K. Phani, and D. F. Styer, J. Stat. Phys. **38**, 413 (1985).

[19]R. B. Griffiths and W. Chou, Phys. Rev. Lett. **56**, 1929 (1986).

[20]W. Chou and R. B. Griffiths, Phys. Rev. B **34**, 6219 (1986).

[21]A. D. Bruce, Adv. Phys. **29**, 111 (1980).

[22]E. Ott, Rev. Mod. Phys. **53**, 655 (1981).

[23]N. Ishimura, J. Phys. Soc. Jpn. **54**, 4752 (1985).

[24]P. Bak and R. Bruinsma, Phys. Rev. Lett. **49**, 249 (1982).

[25]T. De Simone, R. M. Stratt, and J. Tobochnik, Phys. Rev. B **32**, 1549 (1985).